Int. J. Heat Mass Transfer. Vol. 22, pp. 1041–1048
Pergamon Press Ltd. 1979. Printed in Great Britain

HEAT TRANSFER AROUND A CIRCULAR CYLINDER IN A LIQUID-SODIUM CROSSFLOW

RYOJI ISHIGURO, KENICHIRO SUGIYAMA and TOSHIAKI KUMADA
Department of Nuclear Engineering, Hokkaido University, Sapporo 060, Japan

(*Received* 29 *June* 1978)

Abstract—An experimental study was performed to clarify the heat transfer characteristics of liquid sodium flowing uniformly across a circular cylinder. Measurements covered the range of Reynolds numbers from 220 to 16900 and Prandtl numbers from 0.0058 to 0.0073, using three test cylinders of different diameters. A comparison is made between the present results and analytical predictions conducted under the assumption of an inviscid flow field. It was found that there is a considerable discrepancy between the present results and the predictions due to the difference in flow field except at low Peclet numbers.

NOMENCLATURE

a, thermal diffusivity $[m^2 \cdot s^{-1}]$;
Nu_m, average Nusselt number,

$$2q_0 r_0 \Big/ \left(\frac{1}{\pi}\int_0^{\pi} T_{w\theta}\,d\theta\right)\lambda_s;$$

Nu_θ, local Nusselt number, $2q_\theta r_0/T_{w\theta}\lambda_s$;
Pe, Peclet number, $2r_0u_0/a$;
Pr, Prandtl number, ν/a;
q_i, average heat flux at inside surface of sheath $[W \cdot m^{-2}]$;
q_0, average heat flux at outside surface of sheath $[W \cdot m^{-2}]$;
q_θ, local heat flux at outside surface of sheath $[W \cdot m^{-2}]$;
Re, Reynolds number, $2r_0u_0/\nu$;
r, radius [m];
r_i, inside radius of sheath [m];
r_0, outside radius of sheath [m];
r_t, radius to center of thermocouple embedded in sheath [m];
T, temperature difference, $t - t_0$ [K];
T_0, T_n, temperature difference, equation (2), [K];
T_0', T_1', temperature difference, equation (10), [K];
$T_{w\theta}$, local surface temperature difference [K];
t, temperature [K];
t_t, temperature measured by thermocouple embedded in sheath [K];
t_0, upstream temperature [K];
u_0, upstream velocity $[m \cdot s^{-1}]$.

Greek symbols

θ, angle from forward stagnation point [radian];
Θ, angle from forward stagnation point [degree];
λ_c, thermal conductivity of copper $[W \cdot mK^{-1}]$;
λ_s, thermal conductivity of sodium $[W \cdot mK^{-1}]$;
ν, kinematic viscosity $[m^2 \cdot s^{-1}]$;
σ, temperature ratio defined by equation (11).

1. INTRODUCTION

STUDIES on heat transfer to liquid metals have been performed extensively in recent years because of their useful application as a thermal medium. However, research for single phase heat transfer has focused mainly on channel flow problems and little attention has been devoted to boundary layer flow problems.

Since Prandtl numbers of liquid metals are generally small, the thickness of the thermal boundary layer is much greater than the thickness of the hydrodynamic boundary layer. Therefore, the effect of the viscous layer on the heat diffusion process in the case of external flow is limited to only a small portion near the wall. Thus, it may be permissible in such cases to assume an inviscid flow field for the theoretical prediction of heat transfer rates.

Grosh and Cess [1] presented an analytical study of heat transfer with this assumption for low Prandtl number fluids flowing past a single cylinder. Hsu [2] also investigated analytically the problem of heat transfer to a sphere using a treatment similar to that of Grosh and Cess [1]. However, in the actual flow fields around these objects boundary-layer separation inevitably occurs, so that the regular formation of a boundary layer cannot be expected to occur in the region beyond the separation point. Therefore, the previously mentioned analytical methods may not be applied over the whole region from the forward to the rear stagnation points. Grosh and Cess [1] contended that no extreme deviations from their theory occur even within the separated region. This inference was based on the fact that local heat transfer coefficients around a cylinder varied monotonously from a maximum at the forward stagnation point to a minimum at the rear one, a result obtained from an experiment in a tube bundle by Hoe *et al.* [3]. However, the present authors believe that Hoe *et al.*'s [3] result may only corroborate relatively weak hydrodynamic influence on the heat transfer in the separated region due to the large thermal conductivity of liquid metals rather than justify the applicability of the inviscid flow assumption.

On the other hand, Andreevskii [4] measured local and average heat transfer coefficients to the flow of liquid sodium normal to a single cylinder. He also found a monotonous decrease in the local heat transfer coefficients from the forward to the rear stagnation points. However, the average heat transfer coefficients do not agree with the analytical prediction of Grosh and Cess [1] and are about 50% smaller than theory predicts. This discrepancy is too large to be disregarded. Beside the case of a single cylinder, the same kind of discrepancy was observed between the experimental results with a sphere as reported by Witte [5] and the analytical predictions by Hsu [2]. Moreover, since it is not an easy task to obtain experimental data in liquid metals with a good accuracy, the main cause of discrepancy may originate in experimental errors as well as in the simple theoretical assumption. It is of important technological interest to clarify this problem.

The present authors have conducted an experimental study of the heat transfer characteristics of liquid-sodium flow normal to a single cylinder. Some of the results have been reported in previous articles [6, 7]. In the present paper additional measurements are reported from experiments with a new test cylinder and a comprehensive discussion is attempted using all previous data obtained by the authors.

2. EXPERIMENTAL APPARATUS AND PROCEDURE

2.1 *Apparatus*

The experiment was carried out with a sodium loop designed especially for heat transfer measurements. The main line was constructed of 304 stainless steel pipe with 48.6 mm outer diameter. Sodium recirculation rates were obtainable up to $0.2\,m^3 \cdot min^{-1}$ with an electromagnetic pump. Besides the test section, the principal components of the loop were a heater, an expansion tank, two electromagnetic flow meters, a cooler, a drain tank and a cold trap. The flow meters were calibrated by measuring exactly the difference of bulk temperatures of the sodium entering and leaving the heater and the heat input. Since its accuracy depends solely on the heat loss from the heater to the surroundings, guard heaters were attached to compensate for this loss.

Details of the test section are shown in Fig. 1. The cross section, where the test cylinder is set, is 110 mm high and 80 mm wide. A hydrodynamic calming section and a nozzle were prepared to make a uniform velocity profile. A total of six thermocouples for the measurement of sodium upstream temperature were provided in two thin stainless steel thermowells crossing perpendicularly to each other just upstream of mesh screens. Before attaching the test section to the sodium loop, the mesh screens were adjusted to obtain a uniform velocity profile in a water loop.

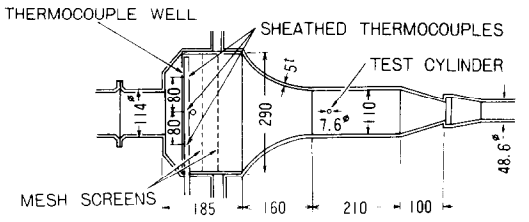

FIG. 1. Details of a test section.

Three test cylinders identified as H-1, H-2, and H-3 with diameters of 7.6 mm, 15 mm and 20 mm, respectively, were used to provide measurements over a wide range of Reynolds numbers. A cross sectional view of the test cylinder with 7.6 mm in diameter is presented in Fig. 2. The heating element is a spiral nichrome wire, 80 mm in length, surrounded by a boron nitride (BN) insulator. Copper

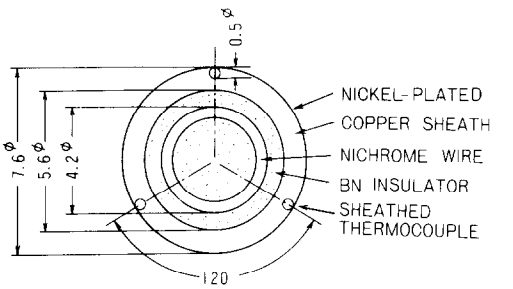

FIG. 2. Cross-sectional view of a test cylinder.

was used as the sheath material, its large thermal conductivity ensuring good accuracy of wall temperature measurement due to the small temperature gradient in the sheath. Three alumel–chromel thermocouples, which were sheathed in a stainless steel tube 0.5 mm in outside diameter, were embedded just below the copper surface. The measuring junctions were set at the longitudinal center of the heating section. The cylinder surface was electroplated with Ni to prevent the dissolution in the liquid sodium of the silver and copper brazing filler compounds, which are described below. Concentricity and uniformity of pitch of the spiral nichrome wire were both confirmed by X-ray photography. The test cylinder was attached to the test section with seals made of silicone rubber packing and asbestos-graphite braid packing so it was possible to rotate the cylinder around its axis. The other two test cylinders had similar setups. The specifications are summarized in Table 1.

Table 1. Summary of data for test cylinders

		H – 1	H – 2	H – 3
Cylinder diameter		7.6	15.0	20.0
Sheath material		Copper		
Thickness of sheath		1.0	2.0	1.0
Plated with		Nickel	Chrome	Nickel
Insulator		BN	MgO	BN
Heating element		Nichrome spiral wire		
Thermo-couple	Sheath dia.	0.5	0.65	0.5
	Number	3	4	4

Unit[mm]

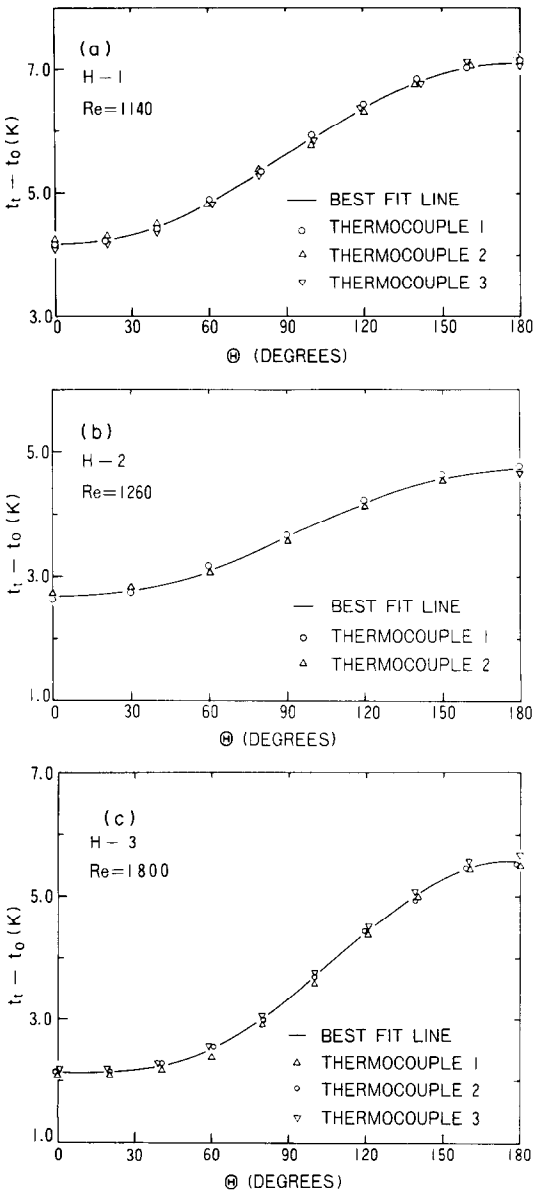

FIG. 3. Examples of temperature distribution measured by thermocouples in test cylinder sheaths.

Two kinds of techniques were employed to fix the sheathed thermocouples under the test cylinder surface. In the case of cylinders H-1 and H-3, the thermocouples were first set tightly in grooves on the copper sheath, then the cylinders were swaged to embed the thermocouples slightly below the surface and to give a smooth outside surface. The small gap left at the tip of the thermocouple after the swaging process was filled with a specially-made silver solder. In the case of cylinder H-2, the grooves were filled merely with the same silver solder after the thermocouples were set. This silver solder is composed of 72% silver and 28% copper by weight. Its thermal conductivity was measured by the step-wise heating method [8] and was found to be 300 and 293 $W \cdot mK^{-1}$ at 473 and 573 K, respectively, which is close to the value of copper. Because the thermal conductivity of the thermocouples is different from that of copper, local distortion of the temperature field in the copper sheath caused by embedding thermocouples is unavoidable. By using the silver solder, we hoped to minimize the distortion of embedding. Furthermore, the error inherent in measuring temperatures due to this local distortion was evaluated by means of a numerical analysis and was found to be less than 0.1 K even in the case of the maximum heat flux in the present experiment.

The diameter of the largest test cylinder, H-3, was 20 mm. The ratio between cylinder diameter and duct height of the test section is 0.18 for this case so that there is a possibility that experimental results were somewhat affected by the flow blockage effect with this cylinder. An examination was made to ensure that the influence was small. To check the magnitude of the effect the heat transfer rate was evaluated under the assumption of inviscid flow fields with and without the duct wall. The result gave about a 2% higher value for the heat transfer rate when the duct wall was in placed.

2.2 *Procedure*

The sodium was passed through the cold trap for purification at a temperature of 420 K for about 8 h before heat transfer measurements began. The cold trap was maintained at this temperature throughout the measurement process. This means that the oxygen content of the sodium in the loop could not be above the saturation value at this temperature. All the thermocouples installed in the test cylinder were calibrated against the thermocouples set in the calming section before and after each run when the cylinder was not being heated. The bulk temperature variation of sodium in the test section during each run was maintained within ± 0.1 K. All e.m.f.'s of the thermocouples installed in the test cylinder, together with those in the calming section, were measured by a digital voltmeter with an accuracy of $\pm 1\,\mu V$. The physical properties of sodium used in the calculations were taken from ANL-7323 [9].

3. EXPERIMENTAL RESULTS AND DISCUSSION

3.1 *Temperature measurements of the test cylinder*

The typical temperature distributions in the sheath material of the test cylinders at the depths of the embedded thermocouple tips are presented in Fig. 3. Figures 3(a–c) correspond to cylinders H-1, H-2 and H-3, respectively. The measurements were made every 20 degrees for H-1 and H-3, and every 30 degrees for H-2. The agreement of values between different thermocouples in each cylinder is fair. As can be seen in the figures, the number of thermocouples used in the actual measurements is different from that presented in Table 1 for H-2 and H-3. Two of the thermocouples in H-2 became nonfunctional in the course of the experiment. This may have been caused by overheating during the brazing process when affixing the thermocouples. In

the case of H-3, the e.m.f. of one of the thermocouples always differed from the others, and it was found afterward that the silver solder covering the measuring tip of this thermocouple had been dissolved by the sodium. Thus, the data obtained from these thermocouples have been omitted.

3.2 *Evaluation of the Nusselt numbers*

As the sheath material was copper, it must be expected that there was a certain amount of circumferential heat conduction through it. On the other hand the insulator material (BN or MgO) has a small thermal conductivity so a uniform heat flux distribution on the inner surface of the copper sheath could be maintained. To assure the latter condition a numerical calculation of the heat conduction of the copper sheath together with the insulated layer was made. The calculation was carried out using the boundary conditions of a uniform heat flux at the location of a spiral nichrome wire and the temperature distribution actually measured at a certain depth from the surface. The results showed that the maximum deviation of the local heat flux at the inner surface of the copper sheath was less than 2% of the average one. As shown in Fig. 3, temperature distributions could be well represented by a finite Fourier series, and the temperature and heat flux distributions at the outer surface of the cylinders were estimated as follows:

The heat conduction equation in the copper sheath is

$$\frac{\partial^2 T}{\partial r^2} + \frac{1}{r}\frac{\partial T}{\partial r} + \frac{1}{r^2}\frac{\partial^2 T}{\partial \theta^2} = 0. \tag{1}$$

The boundary conditions are

$$\left.\frac{\partial T}{\partial r}\right)_{r=r_i} = -\frac{q_i}{\lambda_c}$$

$$T(r_t, \theta) = T_0 + \sum_{n=1}^{N} T_n \cos n\theta \tag{2}$$

$$\left.\frac{\partial T}{\partial \theta}\right)_{\theta=0,\pi} = 0.$$

Integration of equation (1) yields:

$$T(r, \theta) = T_0 - \frac{q_i r_i}{\lambda_c}\ln\left(\frac{r}{r_t}\right) + \sum_{n=1}^{N} T_n\left(\frac{r_t}{r}\right)^n\left(\frac{r^{2n}+r_i^{2n}}{r_t^{2n}+r_i^{2n}}\right)\cos n\theta. \tag{3}$$

Applying this equation to the outer surface of the test cylinder, the surface temperature and heat flux are estimated by:

$$T(r_0, \theta) = T_0 - \frac{q_i r_i}{\lambda_c}\ln\left(\frac{r_0}{r_t}\right) + \sum_{n=1}^{N} T_n\left(\frac{r_t}{r_0}\right)^n\left(\frac{r_0^{2n}+r_i^{2n}}{r_t^{2n}+r_i^{2n}}\right)\cos n\theta \tag{4}$$

$$-\lambda_c\left.\frac{\partial T}{\partial r}\right)_{r=r_0} = \frac{q_i r_i}{r_0} + \lambda_c\sum_{n=1}^{N} nT_n\frac{r_t^n}{r_0^{n+1}}\left(\frac{r_0^{2n}-r_i^{2n}}{r_t^{2n}+r_i^{2n}}\right)\cos n\theta. \tag{5}$$

Thus, the local Nusselt number is

$$Nu_0 = \frac{2q_i r_i + 2\lambda_c\sum_{n=1}^{N} nT_n\left(\frac{r_t}{r_0}\right)^n\left(\frac{r_0^{2n}-r_i^{2n}}{r_t^{2n}+r_i^{2n}}\right)\cos n\theta}{\left\{T_0 - \frac{q_i r_i}{\lambda_c}\ln\left(\frac{r_0}{r_t}\right) + \sum_{n=1}^{N} T_n\left(\frac{r_t}{r_0}\right)^n\left(\frac{r_0^{2n}+r_i^{2n}}{r_t^{2n}+r_i^{2n}}\right)\cos n\theta\right\}\lambda_s}, \tag{6}$$

and the average Nusselt number is defined as follows:

$$Nu_m = \frac{2q_i r_i}{\left\{T_0 - \frac{q_i r_i}{\lambda_c}\ln\left(\frac{r_0}{r_t}\right)\right\}\lambda_s}. \tag{7}$$

3.3 *Discussion*

Figure 4 shows the average Nusselt numbers obtained from the present experiments. The results from each test cylinder appear to be in fair agreement. However, it may be noted that the results of H-3 are somewhat higher than those of the other cylinders. This slight discrepancy may originate in part from the different structure of the cylinder, i.e., the ratio between the thickness of the sheath and the radius of the cylinder being 0.1 for H-3 in comparison to 0.26 of H-1 and H-2. This may cause differences in wall temperature distribution and lead to the discrepancy in the average Nusselt numbers. It could also originate in the blockage of flow, as mentioned in the previous section.

To examine the applicability of the analytical

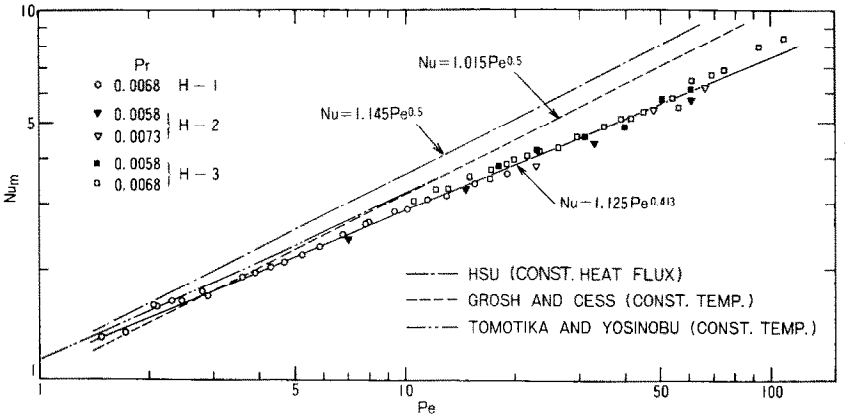

FIG. 4. Average Nusselt numbers.

approach under the assumption of an inviscid flow field, the resulting average Nusselt numbers are compared with the analytical values of Grosh and Cess [1], Hsu [10] and Tomotika and Yosinobu [11] in Fig. 4. In these analytical works the effect of heat conduction in the direction of flow is neglected except in Tomotika and Yosinobu [11]. Since the wall condition of the cylinders in the present experiments is neither uniform in temperature nor uniform in heat flux, it is incorrect to compare them with analytical results which assume such uniformity. However, the comparison does show that the analytical results always give considerably higher values than those of the present experiment except for a range of small Peclet numbers, no matter what the boundary condition is. The best fit line for our experimental values can be formulated as follows:

$$Nu = 1.125Pe^{0.413}. \tag{8}$$

The reason for the difference between the experimental values and the analytical results will be discussed below.

In addition, comparisons between experimental and analytical results were made of the local Nusselt number distributions. As can be seen in Figs 5 and 6, the surface temperature distributions observed in the present measurements for H-1 and H-2 were close to the cosine function $T_0' - T_1' \cos\theta$ for comparatively small Peclet numbers. For this surface temperature condition, Grosh and Cess [1] obtained a closed form solution of the local Nusselt number as follows:

$$Nu_\theta = 1.128Pe^{1/2}(1+\cos\theta)^{1/2} \times \left(\frac{1+\sigma-2\sigma\cos\theta}{1-\sigma\cos\theta}\right), \tag{9}$$

where the circumferential surface temperature variation is represented by

$$T_{w\theta} = T_0' - T_1' \cos\theta \tag{10}$$

and

$$\sigma = T_1'/T_0'. \tag{11}$$

Figure 5 is a comparison of local Nusselt numbers between the present experiment and the theory [1] for the Peclet number 7.8. The experimental Nusselt number is slightly lower but very close to that of Grosh and Cess [1] at the front of the cylinder. However, comparatively large discrepancies are observed between the experimental and theoretical Nusselt numbers elsewhere. The same thing is also true for Peclet number 15 as shown in Fig. 6. In the

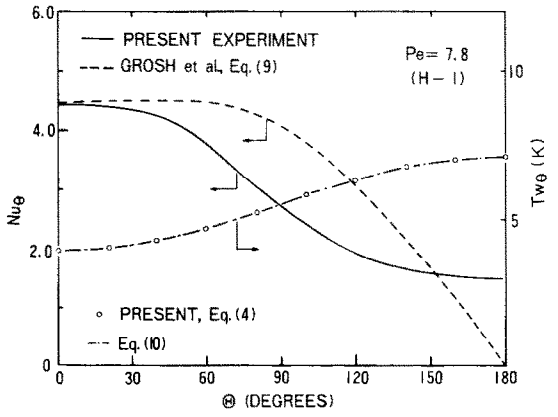

FIG. 5. Comparison of local Nusselt numbers between experimental value and analytical prediction at Peclet number 7.8.

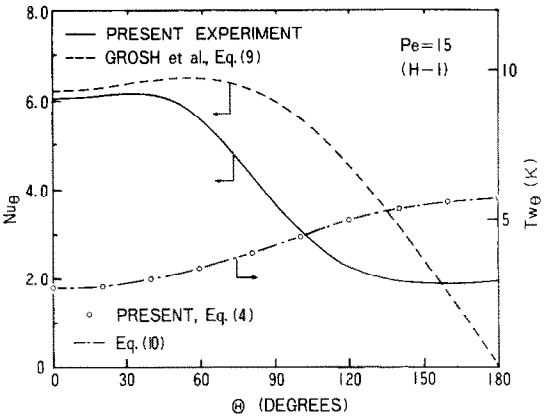

FIG. 6. Comparison of local Nusselt numbers between experimental value and analytical prediction at Peclet number 15.

front of cylinder, the only difference between the inviscid flow assumption and the real field is the existence of a thin boundary layer. So it is natural that the experimental results are close to the analytical values. However, on the surface of the side and rear of the cylinder, the flow pattern of a viscous fluid is very different from an inviscid one because of flow separation and formation of a wake. Therefore, the experimental values of the heat transfer coefficients are expected to give considerably lower values than those of Grosh and Cess [1] as shown in Figs 5 and 6. Grosh and Cess [1] conducted their analytical solution neglecting heat conduction in the direction of flow. Then, the discrepancy in Nusselt numbers in the range of small Peclet numbers may occur because their theory neglects such heat conduction. The authors [12] have evaluated this quantity by numerical methods and found that it is very small even in the case of the Peclet number 7.8. This is also recognized from the fact that the value of Tomotika and Yosinobu [11] is in agreement with the one of Grosh and Cess [1] at about a Peclet number of 8 (Fig. 4).

The authors [12] have also performed a numerical calculation of the viscous flow field for a Peclet number of 7.8. In this calculation the Navier–Stokes equations were solved by an upwind difference approximation with the assumption that a pair of standing vortices exists behind the cylinder. The result gave a separation angle of the boundary layer and a separation stream line similar to those previously reported for some earlier experimental work in the same range of Reynolds numbers. Then, the local Nusselt number was obtained by a numerical computation of the energy equation using this flow field. The temperature distribution actually measured, shown in Fig. 5, was used as the wall condition. A comparison of this numerical result with the corresponding experimental value is presented in Fig. 7. The numerical result of the local Nusselt number gives a value slightly smaller than that of the experimental result but the distributions are very similar.

Because the Prandtl number of liquid sodium is extremely small, it has been said that the heat transfer characteristics may not be greatly affected by differences in the flow field. It may still be true when considering minor differences in the field. However, the calculation of the viscous field suggests that a major alteration of flow field, such as separation of a boundary layer, must considerably affect heat transfer. The discrepancy of the local Nusselt numbers shown in Figs 5 and 6 is, as a matter of fact, attributable to flow separation and wake formation in the actual viscous flow.

It is difficult at the present time to perform the same calculation for large Reynolds numbers because of the unavailability of adequate computer capacity and because of the inapplicability of the standing vortex assumption.

With increasing Reynolds numbers the surface temperature distribution measured in the present experiment cannot be simply represented by equation (10), and the local conformation between the experimental results and the nonviscous analysis become disparate. But the effect of flow separation and wake formation is obvious even looking only at the local Nusselt number distribution of the present experiment in the range of higher Peclet numbers. Figure 8 presents the local Nusselt number and measured temperature distributions at the highest Peclet number ($Re = 1.69 \times 10^4$) obtained by H-3. The local Nusselt number in this case has a minimum value at about 130 degrees from the forward stagnation point. The tendency of local Nusselt numbers to increase in the rear appears clearly for Peclet numbers higher than about 70 in the present experiment. This increase is brought on boundary layer separation, wake, and turbulence, just as in the case of ordinary fluids. Therefore, it appears that the analytical approach under the simple assumption of inviscid flow field is inadequate to predict heat transfer coefficients over the whole region of a cylinder.

If one looks at Fig. 4 again, taking the aforementioned discussion into consideration, it is understood that the asymptotic agreement of the present average Nusselt number with the analytical value of Tomotika and Yosinobu [11] in the range of small Peclet number can be attributed to the weak

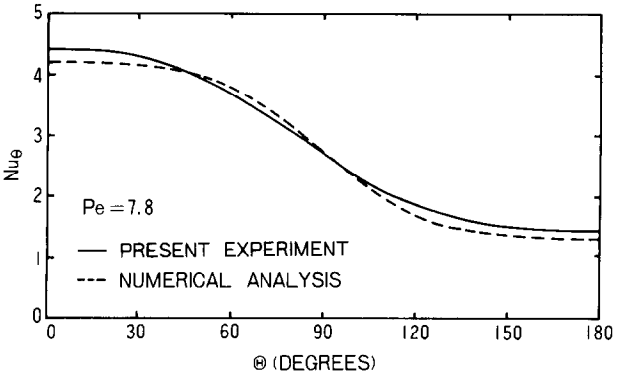

FIG. 7. Local Nusselt numbers by numerical analysis of viscous flow field at Peclet number 7.8.

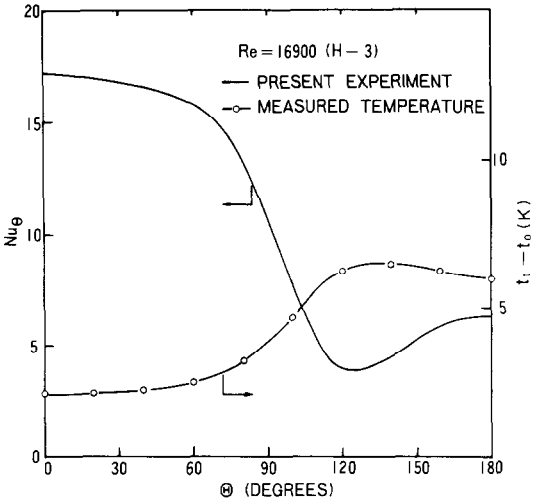

FIG. 8. Distribution of local Nusselt numbers at Reynolds number 1.69×10^4.

influence of the separated region, since the separation point moves to the rear with decreasing Reynolds numbers. In contrast, the departure of the experimental values from the analytical ones for larger Peclet numbers is mainly caused by the increase in the separated region due to the movement of the separation point toward the front of the cylinder.

4. CONCLUSION

The results of the present investigation indicate that local Nusselt numbers vary almost monotomously from the forward stagnation point to the rear in the range of small Reynolds numbers. However, with increasing Reynolds numbers the local Nusselt number achieves a minimum value at a certain location in the rear of the cylinder as in the case of an ordinary fluid. At the front of the cylinder, the present local Nusselt number is in agreement with the analytical value obtained by Grosh and Cess [1] under the assumption of an inviscid flow field, and the analytical treatment of Grosh and Cess [1] is applicable with reasonable accuracy for this region of the cylinder. However, considerably large discrepancies are observed on the side and the rear surface of the cylinder, where a separated region is formed in the actual viscous flow field. These discrepancies of local Nusselt numbers were also identified in a numerical calculation on the assumption of a viscous flow field by the finite difference method. Therefore, the discrepancies are closely related to the difference in flow pattern between inviscid and viscous flows in this region.

The present experimental data for Nusselt numbers are described by equation (8). The surface conditions of the experiment are neither isothermal nor uniform heat flux as mentioned before, but they are close to isothermal for small Peclet numbers and rather close to uniform heat flux for large Peclet numbers. The proposal to use equation (8) as a formula to estimate average Nusselt numbers around a circular cylinder in a liquid-sodium crossflow might not be proper in a strict sense because of this ambiguity in the boundary condition, but it may still be useful for practical purposes.

REFERENCES

1. R. J. Grosh and R. D. Cess, Heat transfer to fluids with low Prandtl numbers for flow across plates and cylinders of various cross section, *Trans. Am. Soc. Mech. Engrs* **80**, 667–676 (1958).
2. C. J. Hsu, Heat transfer to liquid metals flowing past spheres and elliptical-rod bundles, *Int. J. Heat Mass Transfer* **8**, 303–315 (1965).
3. R. J. Hoe, D. Dropkin and O. E. Dwyer, Heat-transfer rates to crossflowing mercury in a staggered tube bank—I, *Trans. Am. Soc. Mech. Engrs* **79**, 899–907 (1957).
4. A. A. Andreevskii, Heat transfer in transverse flow of molten sodium around a single cylinder, *Soviet J. Atom. Energy* **7**, 745–747 (1961).
5. L. C. Witte, An experimental study of forced-convection heat transfer from a sphere to liquid sodium, *J. Heat Transfer* **90C**, 9–12 (1968).
6. R. Ishiguro, T. Kumada, K. Sugiyama and E. Ikezaki, Heat transfer around a circular cylinder in liquid sodium crossflow, *J. Atom. Energy Soc. Japan* **17**, 250–254 (1975). (in Japanese) [This article was translated into English in *Int. Chem. Engng* **16**, 249–253 (1976).]
7. R. Ishiguro, K. Sugiyama and T. Kumada, Heat transfer around a circular cylinder in liquid sodium crossflow (II), *J. Atom. Energy Soc. Japan* **19**, 49–54 (1977). (in Japanese)
8. K. Kobayasi and T. Kumada, A method measuring thermal diffusivity of a small solid disk by step-wise heating, Technol. Rep. Tohoku Univ. **33**, 169–186 (1968).
9. G. H. Golden and J. V. Tokar, Thermophysical properties of sodium, Argonne National Laboratory Report, ANL-7323 (1967).
10. C. J. Hsu, Analytical study of heat transfer to liquid metals in cross-flow through rod bundles, *Int. J. Heat Mass Transfer* **7**, 431–445 (1964).
11. S. Tomotika and H. Yosinobu, On the convection of heat from cylinders immersed in a low-speed stream of incompressible fluid, *J. Math. Phys.* **36**, 112–120 (1957).
12. K. Sugiyama and R. Ishiguro, Heat transfer on a cylindrical surface across uniform flow of liquid sodium, *Trans. Japan Soc. Mech. Engrs* **44**, 3506–3513 (1978). (in Japanese)

TRANSFERT THERMIQUE AUTOUR D'UN CYLINDRE CIRCULAIRE DANS UN ECOULEMENT TRANSVERSAL DE SODIUM LIQUIDE

Résumé—On décrit une étude expérimentale conduite pour clarifier les caractères du transfert thermique du sodium liquide en écoulement autour d'un cylindre circulaire. Des mesures couvrent le domaine des nombres de Reynolds depuis 220 jusqu'à 16.900 et des nombres de Prandtl de 0,0058 à 0,0073, en utilisant trois cylindres de différents diamètres. On fait la comparaison entre les résultats obtenus et les calculs analytiques qui supposent le fluide sans viscosité. On trouve un écart considérable entre les présents résultats et les calculs, à cause de la différence dans le champ des vitesses, sauf aux petits nombres de Péclet.

WÄRMEÜBERGANG AN EINEM VON FLÜSSIGEM NATRIUM QUER ANGESTRÖMTEN KREISZYLINDER

Zusammenfassung—Eine experimentelle Untersuchung wurde durchgeführt, um das Wärmeübergangsverhalten von flüssigem Natrium, das quer zu einem Kreiszylinder strömt, zu ermitteln. Die Messungen wurden für drei Versuchszylinder mit verschiedenen Durchmessern im Bereich der Reynolds–Zahlen von 220 bis 16 900 sowie der Prandtl–Zahlen von 0.0058 bis 0.0073 durchgeführt. Ein Vergleich zwischen den vorliegenden Ergebnissen und analytischen Berechnungen, bei welchen reibungsfreie Strömung angenommen wurde, wird durchgeführt. Außer bei kleinen Peclet–Zahlen wurden erhebliche Unterschiede zwischen den vorliegenden Ergebnissen und den Rechnungen gefunden, was auf Unterschiede in den Strömungsfeldern zurückzuführen ist.

ТЕПЛООБМЕН ПРИ ПОПЕРЕЧНОМ ОБТЕКАНИИ ЖИДКИМ НАТРИЕМ КРУГЛОГО ЦИЛИНДРА

Аннотация — Проведено экспериментальное исследование характеристик теплообмена при равномерном поперечном обтекании круглого цилиндра жидким натрием. Измерения включали диапазон чисел Рейнольдса от 220 до 16 900 и чисел Прандтля от 0,0058 до 0,0073. В экспериментах использовались цилиндры трёх различных диаметров. Проведено сравнение между полученными экспериментальными данными и результатами расчётов, проведенных в предположении о невязком поле течения. Найдено, что полученные данные значительно расходятся с результатами расчётов из-за различия полей течения за исключением случая малых чисел Пекле.